Corrosion Concepts

In dieser Rubrik können Sie, die Leser, praxisorientierte Beiträge zur Diskussion stellen. Es werden Korrosionsprobleme, aber auch Lösungswege und praktische Erfahrungen veröffentlicht. Damit soll der Erfahrungsaustausch unter den Lesern dieses Periodikums zu einer ständigen Einrichtung werden. Vor allem die Praktiker und die „Senior Scientists" sind aufgefordert, von ihrem reichhaltigen Wissen abzugeben. Wir bitten Sie um Ihre Mitarbeit in Form von Beiträgen und Leserbriefen.

In this forum readers will be able to present practical problems for discussion. It is envisaged that these contributions will include not only discussion of general problems and incidents of corrosion but that suggested remedies will also be presented and discussed. It is hoped that this exchange of knowledge and experience will become a permanent feature of this periodical. We are particularly anxious that both Senior Scientists and those with more practical experience will make use of this forum to exchange information, problems and potential remedies.

Long term corrosion behaviour of copper in soil: A study of archaeological analogues

R. Balasubramaniam*, T. Laha and A. Srivastava

The long term corrosion behaviour of copper in soil environment has been addressed by studying two archaeological copper samples. The microstructures of the material of construction of a Chalcolithic (2350BC-1800BC) copper chisel from Balathal and an OCP period (2650BC-800BC) Cu anthropomorphic object have been first characterized by microscopy and the features understood by stereological methods. The equiaxed grain size, coring effects in the grains and the relatively soft matrix of the OCP copper object indicated that it was manufactured by casting. The deformed grains near the surfaces and variation in the microhardness of the sample at different points suggests that the Chalcolithic copper chisel was processed by cold deformation after casting of the square cross section chisel. The surface patina on the two archaelogical copper objects has been characterized by X-ray diffraction. In the case of OCP copper, the green surface patina was analyzed as a mixture composed mainly of cuprite, and minor amounts of malachite and brochantite. In the case of Chalcolithic copper, the patina was composed of sulfates and oxysulfates in the outer layers while the inner layers were rich in copper oxides. The electrochemical behaviour of both the archaeololgical coppers has been characterized and compared with that of a modern Cu sample by potentiodynamic polarization studies. The corrosion rate, determined by Tafel extrapolation technique in 3.5% NaCl solution, of Chalcolithic Cu was only marginally higher than that of modern and OCP Cu. The higher rates of corrosion in case of archaeological coppers have been attributed to the presence of second phase sulfide inclusions.

1 Introduction

The Finnish and Swedish design of spent nuclear fuel package calls for packing the spent fuel in a canister made of spheroidal graphite cast iron, with an outer shield made of copper. The copper shield is responsible for the corrosion protection of the canister [1–3]. The design thickness of the wall of the copper shield is an important consideration and will be based on the maximum corrosion allowance of copper in the disposal conditions. The design life is a minimum 100,000 years [1–3]. The corrosion rates measured in weight loss coupon tests of relatively short duration (7 days) are of the order of 2 μm/year [2, 3]. This corrosion rate would indicate a lifetime of roughly 2500 years for a designed wall thickness of the copper shield of about 50 mm. This is clearly lower than that required for a life of 100,000+ years. Moreover, the actual condition of the material after long term exposure is not

* *R. Balasubramaniam, T. Laha, A. Srivastava*
Department of Materials and Metallurgical Engineering,
Indian Institute of Technology,
Kanpur 208 016 (India)

DOI: 10.1002/maco.200303723

known. Therefore it is important to understand the long-term corrosion resistance of copper in burial conditions. It is in this regard that archaeological analogues can be very useful in understanding and validating theoretical models for long term corrosion of copper. The present study reports material characterization and electrochemical studies conducted on two ancient Indian archaeological copper samples obtained from clay burial conditions. It is anticipated that the present study would provide a few experimental data points that will aid understanding of long term corrosion of copper in burial conditions and support theoretical modeling of the corrosion process.

The two copper samples were obtained from important archaeological excavations conducted recently in India [4–6]. These copper samples will be described briefly. The first Cu sample was from the ochre colored pottery (OCP) period. Although copper hoard implements have been discovered all over India over a fairly wide area, the concentration of these are to be found in Bihar and Western Uttar Pradesh [7, 8]. Ochre colored pottery has been found in the same stratification as the copper hoards [8], thereby placing these copper hoards with the OCP period. *Bharadwaj* places this period between 1100-800 BC [9], while thermoluminescent dates on several OCP sites indicated a time bracket from 2650 BC to 1180 BC [10]. The copper hoards usually contain implements like celts, hatchets, harpoons, spearheads, antennae swords, rings, anthropomorphic figures, etc. Of the numerous copper hoard objects recovered from different North Indian sites, the so-called anthropomorphic figures are the more distinctive and significant [11]. The material of one of the anthropomorphic figures will be reported in the present study. It is important to realize that only fourteen copper anthropomorphic figures were known to the scholarly world [11], of which two were mere fragments, before the discovery of 31 anthropomorphic figures in 2000 AD from an agricultural field near Madarpur village, Thakurdvara tehsil, Moradabad district in Uttar Pradesh [4]. This copper sample will henceforth be called OCP Cu.

The second copper sample was obtained from recent excavations at Balathal in Udaipur District, which is the oldest known village outside the domain of the Indus (Harappan) civilization [5, 6] Radiocarbon dates have provided firm dates between 2600 BC and 1800 BC, thereby firmly placing it as a Chalcolithic site [5]. Balathal is one among the several Chalcolithic sites discovered in the Mewar region of south Rajasthan. The characteristic features of this culture are a variety of ceramics, beads of semi-precious stones and terracotta and animal figurines, copper technology, absence of stone blades and microliths, and an economy based on plant cultivation, animal husbandry, and limited hunting and fishing [5]. The tools and weapons of the Chalcolithic people of Balathal were mainly made of copper. The Harappan influence was noted in the copper implements (barbed arrowheads, knives, chisel, chopper, nail) discovered at Balathal as they were similar to those found in association with Harappans [5, 6]. The Balathal site is close to Ahar ($\sim$ 35 km) from where the inhabitants could have obtained copper implements [5, 6]. It has also been suggested that, as the site is close to copper ore deposits, the Chalcolithic people could have exploited the same [5]. It is interesting to note that small stone blades and tools were completely absent at Balathal, but seen in all other Chalcolithic sites. This clearly suggests that copper metal was plentifully available. Several copper tools and weapons were discovered in the Chalcolithic site of Balathal. In the present investigation, a copper chisel (see Fig. 11 of Ref. 5 for a picture of the copper chisel) from Balathal would also be addressed. This sample will henceforth be called Chalcolithic Cu.

The aim of the present communication is to characterize the long-term corrosion products on these archaeological coppers, and to understand the microstructural features by image analysis and electrochemical behaviour by potentiodynamic polarization studies. A modern pure Cu sample will also be used in the study for comparison purposes.

2 Experimental procedure

The copper samples utilized in the study were obtained with their corrosion product intact. A sample of modern pure Cu, sectioned from a plate, was also utilized in the study for reference purposes. In the case of the OCP copper, a broken arm of one of the figures was utilized for the analysis. The object (broken arm) was curved and the thickness was approximately 3 mm. The object was covered with a light green scale. The Chalcolithic copper sample (chisel) was of square cross-section at one end, tapering down to a smaller flatter cross-section at another end. Its total length was 9 cm and cross-section at the square section was 0.86 cm by 0.86 cm. It was covered with an adherent surface patina, which appeared light green in color.

A small portion of OCP Cu material was sectioned from one corner of the specimen and two sections were prepared for metallographic analysis, one parallel to the surface and another perpendicular to the surface. A small section was made at the square cross section of Chalcolithic Cu sample using a diamond cutter. These samples were utilized for metallographic (optical and scanning electron microscopy) and microhardness measurements. The specimen for metallographic observations was hot mounted. Special care was taken during mounting to maintain the flatness of the sample and the mount. The cross section of the chisel was the section observed on the microscope. The sample was ground and polished very carefully to avoid the reappearance of new scratches. The final polishing was performed with 1 μm diamond paste. The specimen was etched in ferric chloride solution for revealing the microstructure. The microstructures were observed in an optical microscope and a JEOL 840A scanning electron microscope (SEM). Elemental analyses were obtained at several different locations in the sample using a JEOL 8000 JXA electron probe microanalyzer (EPMA). The microhardness variation across several sections were measured using a Carl Zeiss Jena 160 microhardness tester.

The image from the optical microscope (Axiolab A, Zeiss, Germany) were grabbed in a digital camera (CE, Japan) and later used in an image analysis program (Image-Pro Plus 4.1, Media Cybernetics, USA). The volume fraction of the inclusions and the grain sizes were estimated. In order to measure the volume fraction, 30 fields of view (FOV) were captured (at a magnification of 200X) and analyzed. A 15×11 grid was imposed on each of the FOVs. The number of points falling in the feature of interest was calculated manually and divided by the total number of grid points to provide the volume fraction. The linear intercept method was used for measuring the grain size. Thirty FOVs were captured and nine test lines were imposed on each of the FOVs using the software. The number of intersections between the test lines and the grain boundaries were counted. The total length of test lines divided by the total

number of intersection points provided the grain size. Thirty FOVs help to minimize statistical error.

In order to understand the nature of the scale, X-ray diffraction (XRD) patterns were obtained from the surface of the OCP Cu. The XRD experiments were conducted in a Rich-Seifert X-ray Diffractometer, taking special care to maintain the same conditions for all the experiments (constant current of 20 mA and voltage of the X-ray tube 30 kV). The wavelength of the radiation used was Cu K_α (1.54184 Å). As the Chalcolithic sample possessed a thicker corrosion product layer, a sample was specifically sectioned from the chisel for careful XRD analyses. XRD patterns were first obtained from all the surfaces of the Chalcolithic Cu section, and later, were again determined after slightly polishing off the surface layers using fine emery paper. The XRD patterns were analyzed by using DIFFRAC^{plus} Software (Bruker Advanced X-Ray Solutions) and JCPDF database [12]. It was not easy to identify the peaks due to high amount of noise and texturing and in this regard the DIFFRAC^{plus} software was very useful in removing some noise and texturing effects.

In case of electrochemical studies, a sample was sectioned from the Chalcolithic Cu chisel and was mounted in a cold setting epoxy, after soldering a conductive wire to it. One of the OCP Cu samples that was used for the microstructural study (i.e. the sample obtained parallel to the surface) was removed from the mount and re-mounted in a cold setting epoxy, after soldering a conductive wire to it. Electrochemical polarization experiments were conducted utilizing a potentiostat (263A Perkin Elmer, USA). Polarization studies were carried out in freely aerated 3.5 wt % NaCl solution. The samples were polished to 4/0 grade emery paper finish and the surfaces were cleaned using distilled water and acetone before the start of each experiment. A round-bottom polarization cell, with graphite counter electrodes and saturated calomel electrode (SCE) (+ 241 mV vs standard hydrogen electrode) reference electrode was used in the electrochemical study of the Chalcolithic Cu. A flat cell with platinum as the counter electrode and Ag/AgCl in saturated KCl (SSC) (+ 198 mV vs SHE) as the reference electrode was used in case of the OCP Cu. Potentiodynamic polarization experiments were performed to compare the electrochemical behavior of the samples with modern Cu. All potentiodynamic polarization experiments were conducted after stabilization of free corrosion potentials. Corrosion rates were determined by the Tafel extrapolation procedure. A scan rate of 1 mV/s was used for potentiodynamic polarization experiments and 0.166 mV/s for Tafel extrapolation, as per ASTM standards [13].

The microhardness variation, as a function of distance from the surface, was obtained from the surfaces.The microhardness experiments were performed in a Carl Zeiss Jena 160 microhardness tester. The hardness was measured across a line perpendicular to the surface, from the edge progressing towards the middle of the specimen, at systematic intervals. Six profiles were recorded from each of the four specimen surfaces and the average estimated for each data point.

3 Results and discussion

The results of the present study will be presented and discussed in the following sections.

3.1 X-ray diffraction analysis

The XRD patterns obtained from all the four faces of the as-received Chalcolithic Copper were similar, barring some very minor variations. This indicated that the environment, to which the copper chisel was exposed to, was uniform, and the relatively uniform chemical nature of the exposed four faces of the copper chisel. A typical diffraction pattern obtained from the surface is shown in Fig. 1a. The peaks were compared with that of the common corrosion products of Cu [12]. Apart from peaks due to the substrate Cu, all the other peaks could be indexed unambiguously to specific corrosion products. It was firmly concluded that the major corrosion products on the surface of the sample were hydrated copper sulfates and oxysulfates (Fig. 1a). The specific phases identified were $Cu_4(SO_4)(OH)_6 \cdot 2H_2O$ posnjakite (JCPDF 43-0670), $CuSO_4 \cdot H_2O$ (JCPDF 80-0392), $Cu_3(SO_4)_2(OH)_2$ (JCPDF 37-0526) and $Cu_3(SO_4)_2(OH)_2 \cdot 4H_2O$ (JCPDF 37-0525).

The XRD patterns of the Chalcolithic Cu surfaces were redetermined after a slight polishing procedure with emery paper. The XRD patterns from all the surfaces were again similar. A typical pattern after the slight polishing procedure is shown in Fig. 1b. Analysis of these XRD patterns revealed that the phases were primarily copper oxide phases (Fig. 1b). The identification of peaks corresponding to $Cu_{64}O$ is interesting because it indicated that a suboxide, rich in Cu, was present and this must be present below the

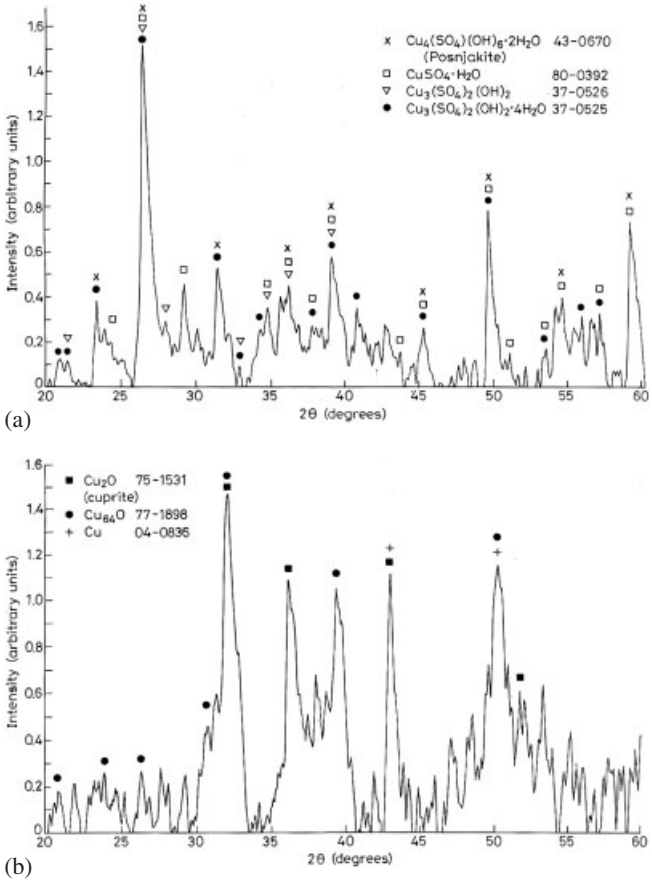

Fig. 1. X-ray diffraction pattern from the surface of the Chalcolithic Cu sample (a) before, and (b) after slightly polishing the surface of the sample. The peaks corresponding to the identified phases have been marked in both the patterns

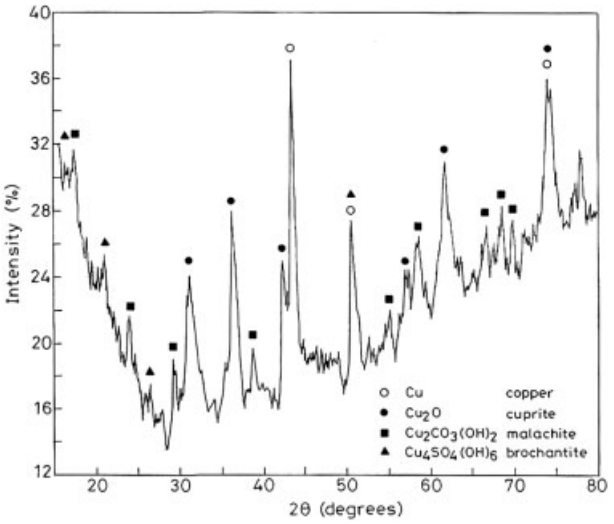

Fig. 2. X-ray diffraction pattern from the surface of the OCP Cu anthropomorphic figure. The peaks corresponding to the identified phases have been marked

cuprite (Cu_2O) phase in the patina. The peaks from the Cu matrix were relatively more intense than in the earlier case (Fig. 1a). This indicates that the information provided by Fig. 1b would apply to the nature of corrosion products near the metal-scale interface. The XRD patterns before polishing and after polishing of the sample surface helps in understanding the sequence of formation of corrosion products. The results of the analysis agree with the known general behaviour for corrosion of copper in soil environments [14]. In the corrosion of copper in soil (and also atmospheric environments), the first product to form is cuprite. In the presence of S in the environment, the formation of sulfates and oxysulfates is favored and these phases are generally found above the copper oxide containing layer. This behaviour has been also observed in the case of the Chalcolithic copper chisel.

The X-ray diffraction pattern obtained from the surface scale of the OCP Cu object is presented in Figure 2, along with the indexed peaks of the corrosion products. Based on the peak intensities, it can be concluded that the major corrosion product was cuprite (Cu_2O, JCPDF 34-1354), while the minor corrosion products were malachite ($Cu_2CO_3(OH)_2$, JCPDF 41-1390 and 10-0399) and brochantite ($Cu_4SO_4(OH)_6$, JCPDF 43-1458). The identification of minor amounts of malachite and brochantite is indicative of the soil corrosion of the OCP Cu object. It is interesting to note that malachite is not a common atmospheric corrosion product of Cu and is sometimes found as a patina constituent of ancient statues [14].

3.2 Microstructural analysis

3.2.1 OCP copper

Optical microscopy indicated several macrodefects in the cross section of the specimen, like wide cracks (Figure 3a). The grain structure was equiaxed and a non-uniform distribution of second phase particles was observed in the matrix (Figure 3b). There were several grains in the structure where straight annealing twins were present. This indicated that the structure had not been deformation processed because annealing twins were straight and not bent [15]. Secondly, the

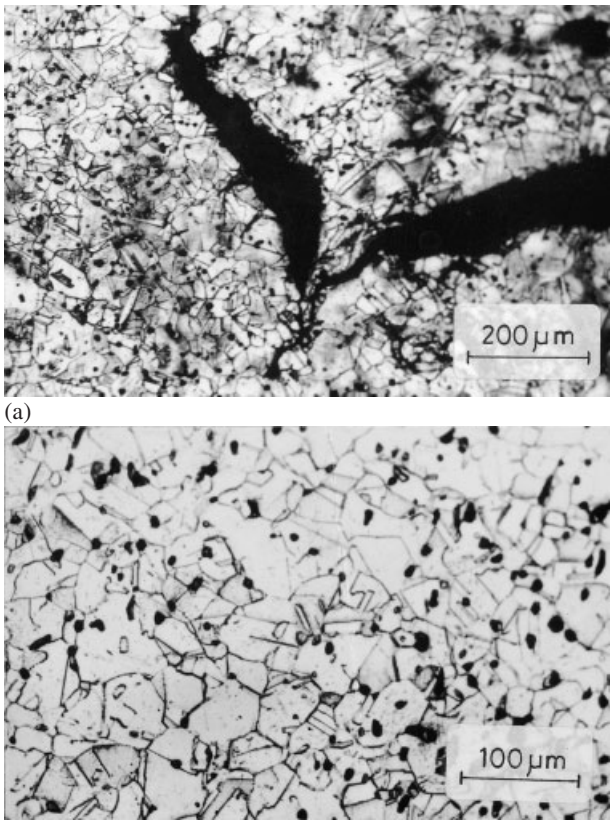

Fig. 3. Optical micrograph of the OCP Cu sample showing (a) presence of a macrodefect (crack). Notice the relatively uniform grain structure, and (b) equiaxed grains and entrapped slag inclusions of spherical shape. The presence of straight annealing twins in some of the grains can be noticed in (b). The microstructure (b) represents a typical cast structure

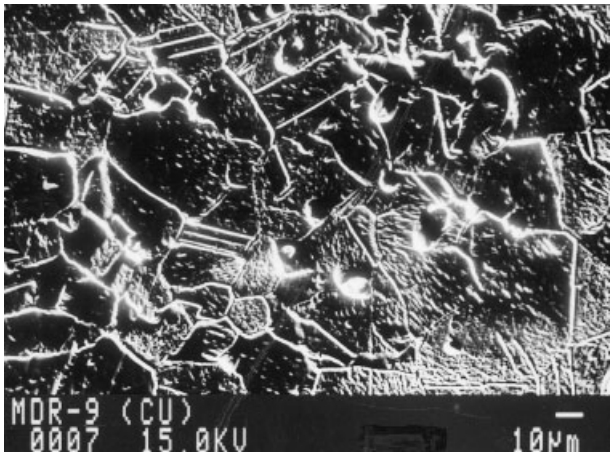

Fig. 4. SEM micrograph of OCP Cu showing spherical-shaped sulfide inclusions in almost pure copper matrix. Coring can be observed in some grains

second phase particles were rounded and spherical in shape and not elongated, further proving the absence of any deformation processing [15]. The equiaxed grains further did not exhibit any indications of deformation (Figure 3b). The equiaxed structure was revealed in both the sections (parallel and perpendicular to the surface), which strongly suggested the casting route for the manufacture of the object. The grain

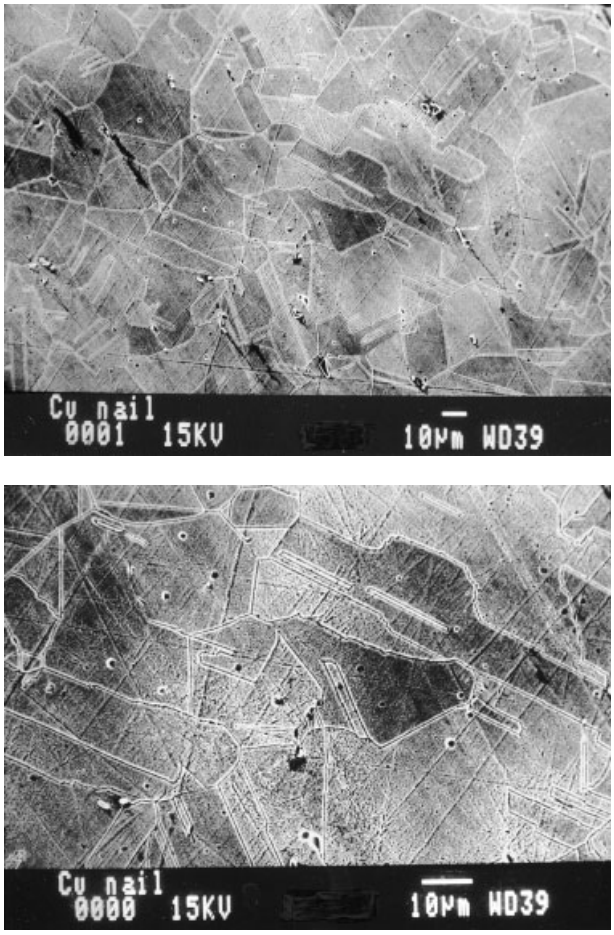

Fig. 5. SEM micrographs obtained from the center of the Chalcolithic copper chisel cross section showing entrapped second phase spherical inclusions inside the grains. Annealing twins can also be observed in some of the grains

size was not strictly uniform. A detailed analysis of the grain sizes in the microstructures will be provided later.

Scanning electron microscopy of the polished and etched sections also revealed similar features (Figure 4). Coarse dendritic structures (fernlike growth) were noticed in some of the grains. As faster cooling results in finer dendrites, the presence of relatively coarser dendrites indicated the relatively lower cooling rates after the casting process. Features indicative of coring (and the presence of dendrites) confirmed that the object was a cast structure. There was no preferential grain growth, like columnar growth, thereby eliminating chill casting of the object. Moreover, the presence of dendrites negates annealing [15] and therefore, the objects were cast structures. The second phase particles were nearly rounded in most of the cases (see Figures 3b and 4), thereby indicating that the material was molten and then cast into moulds. In the process, the second phase particles assume spherical shapes based on surface energy considerations. This aspect of coagulated second phase particles in ancient Cu objects indicating casting of Cu object has also been addressed elsewhere in detail [16]. The results of the present study are in conformity with a detailed study of copper hoard implements by *Agrawal* et al. [17], who had concluded that the objects were cast in closed moulds. They also noted the skill of the metal casters because casting of pure Cu is a difficult process. Finally, it was confirmed in the present study that the objects were manufactured by the casting process by visual observation of depressions on the surface of the objects, indicative of shrinkage of the material after they were cast into shape.

3.2.2 Chalcolithic copper

The microstructure of the sample was analyzed in an optical and a scanning electron microscope (SEM). Microstructural analysis revealed an almost equiaxed microstructure containing entrapped second phase inclusions (Fig. 5). The entrapped second phase inclusions were generally spherical in shape. Some of these inclusions, especially those near the edge of the sample, were deformed. The microstructure was not completely homogeneous. In the middle of the sample, the grains were equiaxed (Fig. 5a) and some of the grains revealed annealing twins (Fig. 5b). At ambient temperatures, copper deforms by slip, while deformation by twinning is possible only at low temperatures. Moreover, deformation twins appear jagged, unlike the twins seen in Fig. 5b. Therefore, the twins noticed in Fig. 5b are annealing twins. This provides the first indication that the object was first cast into shape. The etching in some grains was non-uniform due to coring effects, similar to that observed in an OCP Cu object studied above. These coring effects result during the initial casting of the object. As they were not removed in the sample, it proves that the Cu chisel has been initially cast into shape.

The microstructure from near two opposite surfaces of the sample, however, was quite different (Fig. 6a–c). The grains were deformed compared to the grains in the interior. These microstructures reveal a cold worked structure with numerous slip bands. The important conclusion that can be deduced from these microstructures is that the initially cast chisel has been cold worked only on two sides to provide the final shaping operation to the chisel. It is also interesting to note the possible reason why the shaping operation was provided on only two opposite faces and not on all the four faces. This was because the chisel was finally hammered to the shape of a flat edge and deformation of only two faces was required for this purpose. Therefore, based on the microstructural observations, the Chalcolithic Cu chisel was initially cast and later was cold worked on two opposite sides to produce the shape of the chisel.

Interestingly, there were no stress corrosion cracks emanating from the edges or corners. Some features of corrosion attack can also be observed in the microstructures obtained from the edges (Fig. 6). The microstructures (Fig. 6a and Fig. 6b) from near the edge of the sample show the corrosion layer on the right side of the photograph. The incursion of corrosion products into the matrix appears to occur along grain boundaries of the underlying matrix. (see Fig. 6b and 6c). The intergranular nature of corrosion attack is understandable because of the higher-energy state of the material at these locations. Nevertheless, it is also important to note that the incursion of corrosion products along the grain boundaries was not deep enough to warrant the use of the term pitting to describe this kind of environmental corrosion. A complementary conclusion is the lack of any environmentally induced cracking in this material. This is understandable because dangerous chloride ions were not present in the soil environment to which the chisel was exposed. This conclusion is based on the absence of chlorides in the surface patina. (Fig. 1a and Fig. 1b). Therefore in the environments where chloride ions are excluded, microstructural investigations on archaeological copper provide that there is no danger of stress corrosion cracking. This

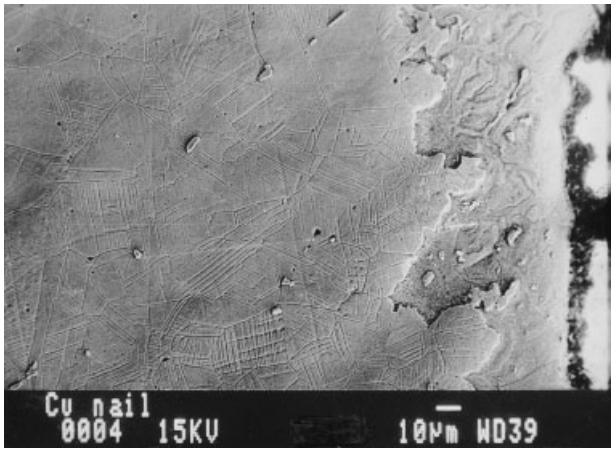

(a)

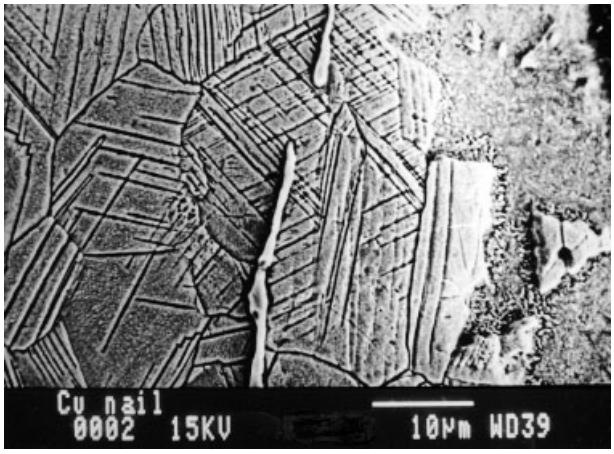

(b)

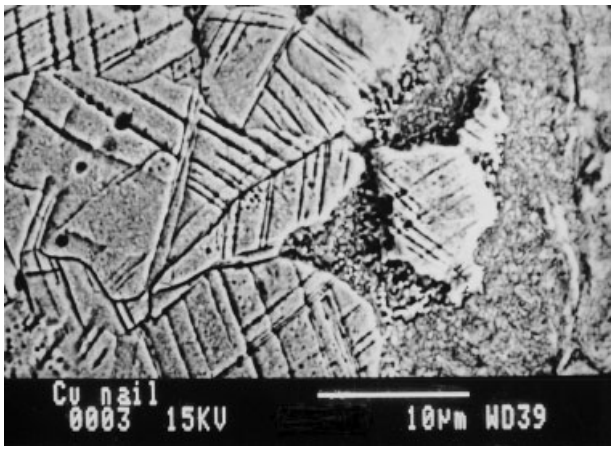

(c)

Fig. 6. SEM micrographs photographed from one of the edges of the Chalcolithic copper chisel, showing deformed grains and incursion of corrosion products along grain boundaries. The corrosion layer is on the right side of the photograph. Elongated bright slag inclusion can also be seen in (b)

has implications in selection of Cu as the material for long-term nuclear storage canisters [1, 2].

The bright contrast obtained from some of the entrapped inclusions in both samples using back scattered electron imaging in the SEM indicated that they must be rich in Pb. The dark-appearing second phase inclusions in the OCP Cu were analyzed in an electron probe microanalyzer as sulfides of Cu, while the same in Chalcolithic Cu was analyzed as sulfides of Cu and Fe. The composition of the OCP object was almost pure Cu, with minor impurities of C and Sb. In the case of Chalcolithic Cu, the composition of the matrix was essentially pure Cu with trace amounts of As and Sn. The co-relation of the composition of the entrapped slag inclusions in these coppers and their mode of extraction has been discussed in detail elsewhere [18, 19].

The volume fraction of second phase inclusions and the grain size were determined as per the procedure discussed earlier. The image analysis results are tabulated in Table 1. The volume fraction of second phase inclusions was almost similar in both the OCP Cu sections. The grain size of the OCP Cu from both the sections was also comparable, therefore attesting to the casting method of production of the anthropomorphic figure. The volume fraction of inclusions in the archaeological coppers was relatively low and almost similar to each other, thereby suggesting similarities between the OCP and Chalcolithic coppers. The grain size of Chalcolithic Cu was slightly lower compared to modern Cu or OCP Cu.

3.3 Microhardness

Microhardness readings were obtained from several locations in the matrix of the OCP copper sample and the results indicated a relatively soft matrix (hardness in the range of 65 to 80 kg/mm^2). The relationship of microhardness and grain size with the possible temperature range of working for the case of Cu has been addressed in detail, recently [16]. In the case of OCP copper, grain sizes in the range of 30 to 40 µm and hardness in the range of 65 to 80 kg/mm^2 were obtained. These specifications are well within the range for cast structures without any further deformation [16].

A different behaviour was observed in the case of Chalcolithic copper sample. Unlike the OCP copper, the microhardness was not constant in the matrix. The variation of microhardness as a function of distance into the material from the surface is shown in Fig. 7. The hardness profiles were almost constant on two opposite faces, while on the other two faces, the hardness was much higher near the surface, which progressively decreased on moving towards the interior (Fig. 7). The hardness of the matrix in the center was almost similar for all profiles. The microhardness measurements confirmed deformation on two of the surfaces. On the other opposite two surfaces, there was no significant variation in the hardness from the surface to the middle of the specimen.

3.4 Electrochemical behaviour

The copper samples used in the study were very old samples, of conservative age between 3800 and 2800 years. From microstructural analysis it has been found that the degree of corrosion was not severe and moreover, stress corrosion cracking was not evident from the surfaces of the sample. Electrochemical characterization will reveal information about its corrosion properties, which can be compared with that of modern Cu.

The free corrosion potential of the Chalcolithic and OCP copper samples stabilized relatively quickly on immersion in the electrolyte. This indicates that equilibrium corrosion conditions (i.e. supporting anodic and cathodic reactions) are established fairly quickly on the surface of the archaeological samples. This behaviour was similar to that observed for modern Cu. Therefore, the entrapped slag inclusions in the

Table 1. Volume fraction of inclusions and grain size, calculated by image analysis

Copper Sample	Volume fraction			Grain size		
	% V_v	Std. Dev.	% error (±)	Size (μm)	Std. Dev.	% error (±)
Modern	–	–	–	19.47	1.57	2.95
Chalcolithic	2.78	0.59	7.68	14.10	2.66	6.88
OCP	2.11	0.90	11.02	19.50	3.79	7.09

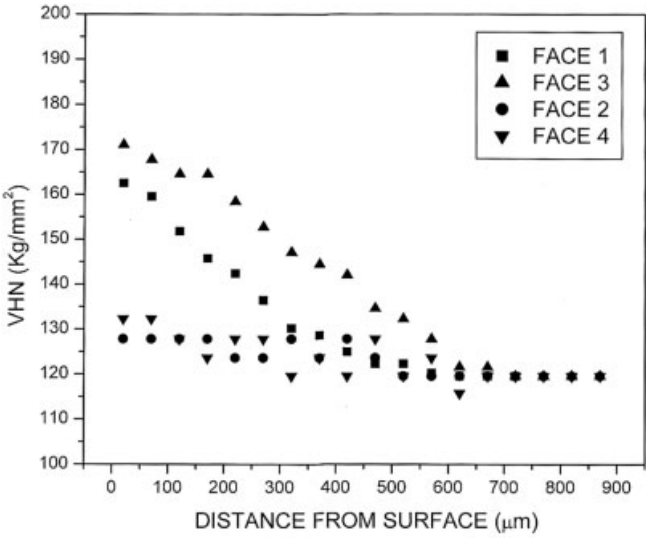

Fig. 7. Variation of microhardness as a function of distance into the surface of Chalcolithic copper sample from all the four surfaces

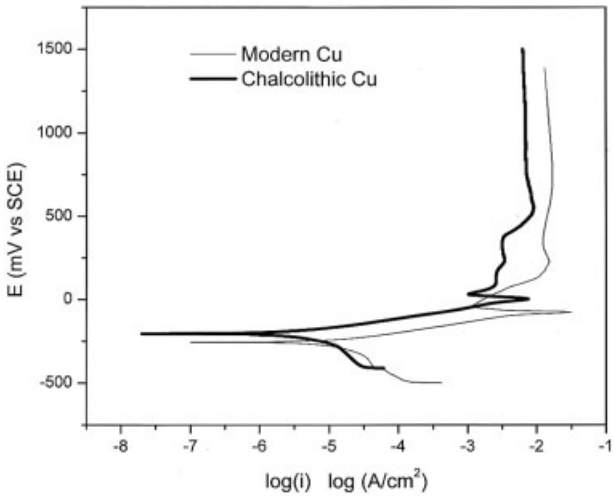

Fig. 8. Potentiodynamic polarization curves for modern and Chalcolithic coppers in aerated 3.5 wt % NaCl solution

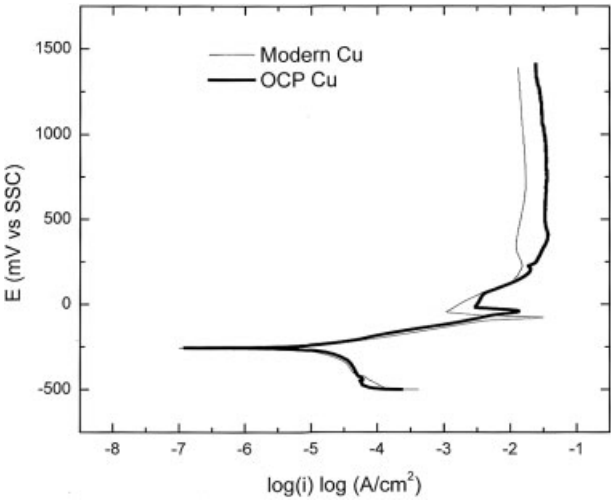

Fig. 9. Potentiodynamic polarization curves for modern and OCP coppers in aerated 3.5 wt % NaCl solution

archaeological coppers do not deleteriously affect the establishment of equilibrium corrosion conditions on the surface, which is understandable as the volume fraction of entrapped inclusions was relatively low (Table 1). The potentiodynamic polarization curves for modern and Chalcolithic Cu samples in 3.5 wt % NaCl solution are compared in Fig. 8, while that for OCP Cu and modern Cu in Fig. 9. All the copper samples exhibited similar electrochemical behaviour in the NaCl solution. The polarization behaviour of modern Cu was in excellent agreement with published data [20]. The surface film that formed at anodic potentials was very stable because no pitting was observed even up to + 1400 mV vs SCE. A thin adherent surface film was visually observable in all the samples even after removal from the solution, at the end of each experiment. The various potentials like zero current potential, primary passivation potential, etc. were similar for the samples indicating that the entrapped slag inclusions did not significantly affect the polarization behaviour.

Table 2. Results of Tafel extrapolation experiments

Copper Specimen	β_c (mV/dec)	β_a (mV/dec)	i_{corr} (μA/cm²)	Corrosion rate (μm /y)	Zero Current Potential (mV vs SCE)
Modern	−26	21	0.49	55	− 226
Chalcolithic	− 32	37	0.63	175	− 172
OCP	− 28	37	0.67	185	− 194

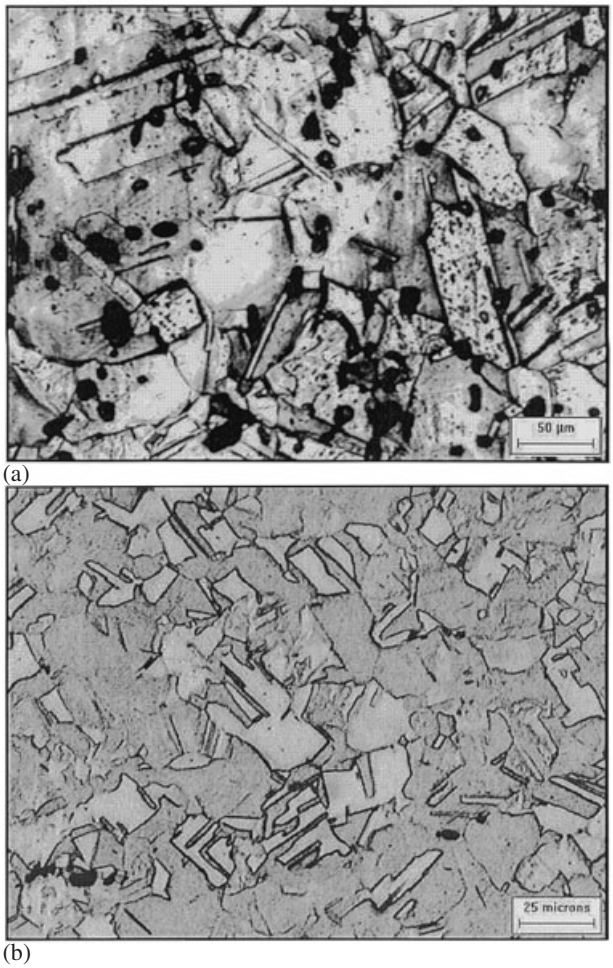

Fig. 10. Optical micrographs of (a) OCP Cu and (b) modern Cu surfaces that were exposed in the potentiodynamic polarization studies

The major difference between the samples was the presence of second phase inclusions in the case of the archaeological Cu samples. The optical micrographs of the faces of OCP Cu and modern copper that were exposed in the potentiodynamic polarization study are shown in Fig. 10. It was anticipated that the presence of second phase inclusions would affect the corrosion rates. Table 2 presents the results of Tafel extrapolation method for modern, Chalcolithic and OCP coppers. The anodic and cathodic Tafel slopes were almost similar for the three samples, which is reasonable. The corrosion rates of Chalcolithic Cu sample (175 µm/y) and OCP Cu sample (185 µm/y) were higher than that of modern Cu (55 µm/y). The corrosion rate for modern Cu agreed well with the published corrosion rate for Cu in seawater (25 – 127 µm/y) [21]. In the case of both archaeological coppers, the second phase slag particles appear to have slightly enhanced the dissolution tendencies, which could probably be due to galvanic coupling action of the Cu matrix with the slag inclusions. It is to be noted that the sulfides are electrically conducting and they aid in the establishment of local galvanic cells [22]. The effect of the inclusions was not significant because the volume fraction of inclusions was relatively low and, moreover, they were not interconnected but widely dispersed (Fig. 10).

4 Conclusions

The microstructures of the material of construction of a Chalcolithic (2350BC-1800BC) copper chisel from Balathal and an OCP period (2650BC-800BC) Cu anthropomorphic object have been characterized by microscopy and the features understood by stereological methods. The equiaxed grain size, coring effects in the grains and the relatively soft matrix of the OCP copper object indicated that it was manufactured by casting. The equiaxed microstructure in the center, deformed grains and inclusions near the surfaces and variation in the microhardness of the sample at different points suggests that the Chalcolithic copper chisel was processed by cold deformation after casting of the square cross section chisel. The surface patina on the two archaeological copper objects has been characterized by X-ray diffraction. In the case of OCP copper, the green surface patina was analyzed as a mixture composed mainly of cuprite, and minor amounts of malachite and brochantite. In the case of Chalcolithic copper, the patina was composed of sulfates and oxysulfates in the outer layers while the inner layers were rich in copper oxides. The electrochemical behaviour of both the archaeololgical coppers has been characterized and compared with that of a modern Cu sample by potentiodynamic polarization studies. The corrosion rates, determined by Tafel extrapolation technique in 3.5% NaCl solution, of Chalcolithic Cu and OCP Cu was higher than that of modern Cu. The higher rates of corrosion in case of archaeological coppers have been attributed to the presence of second phase sulfide inclusions.

5 Acknowledgements

The authors would like to thank Professor *V. N. Misra* and the Archaeological Museum, Deccan College, Pune for providing the Chalcolithic copper chisel sample, and Dr. *D. V. Sharma* and the Archaeological Survey of India, for providing the OCP copper anthropomorphic sample. RB would like to thank *Bo Rosborg* and *Graham Quirk* for useful discussions and careful suggestions. RB would like to acknowledge the equipment grant (potentiostat) from the Alexander von Humboldt foundation.

6 References

[1] L. Werme, P. Sellin, The Performance of a Copper Canister for Geologic Disposal of Spent Nuclear Fuel in Granitic Rock, Proceedings of the *International Workshop on Prediction of Long Term Corrosion Behaviour in Nuclear Waste Systems*, European Federation of Corrosion, Series 42, **2003**, in press.
[2] M. Bojinov, J. Hinttala , P. Kinnunen, T. Laitinen, C. Lilja, K. Mäkelä, T. Saario, Approaches Chosen to Predict the Effect of Different Forms of Corrosion on Copper in Disposal Conditions of Spent Fuel, *ibid*.
[3] B. Rosborg , O. Karnland, G. Quirk, L. Werme, Measurements of copper corrosion in the LOT project at the Äspö Hard Rock Laboratory, *ibid*.
[4] D. V. Sharma, V. N. Prabhakar, *Indian Archaeology – A Review,* **2003**, in press.
[5] V. N. Misra, V. Shinde, R. K. Mohanty, K. Dalal, A. Mishra, L. Pandey, J. Kharakwal, *Man and Environment* **1995**, *20*, 57.
[6] V. N. Misra, V. Shinde, R. K. Mohanty, L. Pandey, J. Kharakwal, *Man and Environment* **1997**, *22*, 35.
[7] B. B. Lal, *Ancient India* **1951**, *7*, 20.
[8] B. B. Lal, *Puratattva* **1971 – 72**, *5*, 46.

[9] H. C. Bharadwaj, *Aspects of Ancient Indian Technology*, Motilal Banarsidass, New Delhi **1979**, 1–23.
[10] K. N. Dikshit, in: *Essays in Indian Protohistory* (Eds. D. P. Agarwal and D. K. Chakraborty), New Delhi **1979**, 285–299.
[11] K. Kumar, *Journal of the Indian Society of Oriental Art, New Series* **2000**, *22&23*, 27.
[12] JCPDS Powder Diffraction Files, *PCPDFWIN Software*, Joint Committee on Powder Diffraction Standards – International Centre for Diffraction Data, Swarthmore, USA **2001**.
[13] American Society for Testing of Materials, *Metals Test Methods and Analytical Procedures*, Annual Book of ASTM Standards, Volume 3.02, Section 3, Philadelphia, USA **1987**.
[14] C. Leygraf, T. Graedel, *Atmospheric Corrosion*, Wiley-Interscience, New York **2000**, 140–148.
[15] D. A. Scott, *Metallography and Microstructures of Ancient and Historic Metals*, Archetype Books, London **1991**, 5–10.
[16] N. V. Ryndina, I. J. Ravich, *Bulletin of the Metals Museum* **2001**, *34*, 16–21.
[17] D. P. Agrawal, R. V. Krishnamurthy, S. Kusumgar, *Man and Environment* **1978**, *2*, 41.
[18] R. Balasubramaniam, M. N. Mungole, V. N. Prabhakar, D. V. Sharma, D. Banerjee, *Man and Environment* **2002**, *26*, 89.
[19] R. Balasubramaniam, M. N. Mungole, V. N. Prabhakar, D. V. Sharma, D. Banerjee, *Indian Journal of History of Science* **2002**, *37*, 1.
[20] K. R. Trethewey, J. Chamberlain, *Corrosion for Students of Science and Engineering*, Longman Scientific, Harlow **1988**, 92.
[21] F. L. LaQue, *Marine Corrosion - Causes and Prevention*, John Wiley, New York **1975**, 146.
[22] G. Wranglen, *Corrosion Science* **1969**, *9*, 585.

(Received: April 29, 2003) W 3723